FRII SOURCES AT $Z > 0.5$: X-RAY PROPERTIES OF THE CORE AND EXTENDED EMISSION

E. Belsole[1], J.H. Croston[2,3], D.M. Worrall[1], and M. J. Hardcastle[3]
[1]H.H. Wills Phyisics Laboratory, University of Bristol, Tyndall Avenue, Bristol BS8 1TL, UK
[2]Service d'Astrophysique, bat 709 CEA- Saclay, L'orme des Merisiers, 91191 Gif sur Yvette Cedex, France
[3]School of Physics, Astronomy and Mathematics, University of Hertfordshire, College Lane, Hatfield, Hertfordshire AL10 9AB, UK

ABSTRACT

Active galaxies are the most powerful engines in the Universe for converting gravitational energy into radiation, and their study at all epochs of evolution is therefore important. Powerful radio-loud quasars and radio galaxies have the added advantage that, since their radio jets need X-ray-emitting gas as a medium in which to propagate, the sources can be used as cosmological probes to trace significant atmospheres at high redshift. The radio emission can be used as a measure of source orientation, and sensitive X-ray measurements, especially when used in combination with multi-wavelength data, can be used to derive important results on the physical structures on a range of sizes from the cores to the large-scale components. In this paper we present new results on a significant sample of powerful radio galaxies and quasars at $z > 0.5$, drawn from the 3CRR catalogue and selected to sample a full range of source orientation. Using high-quality observations from *XMM-Newton* and *Chandra*, we discuss the X-ray properties of the cores, jets, lobes and cluster gas, and, through the incorporation of multi-wavelength data, draw conclusions about the nature of the emission from the different components.

Key words: active galaxies, radio galaxies, high redshift, quasars, general, X-ray, synchrotron, inverse Compton.

1. INTRODUCTION

Powerful ($P_{178\mathrm{MHz}} > 5 \times 10^{24}$ W s^{-1} Hz^{-1}) radio sources are visible across the Universe and can thus be used to probe a number of physical conditions at high redshift, from accretion processes to Active Galactic Nucleus (AGN) environments at early epochs. On small scales, X-ray emission from the central AGN can be used to probe the process of converting gravitational energy into radiation, as spectral and variability studies have shown that at least some of the X-ray emission comes from regions very close to the central engine. At least part of the X-ray emission is expected to be anisotropic as a result of relativistic beaming and anisotropic absorption. In particular, Unification Models explain the observed differences among AGNs as the result of their orientation with respect to the line of sight (e.g. Barthel 1989; Urry & Padovani 1995), and an optically thick obscuring torus is invoked to hide the nucleus of objects (namely radio galaxies) viewed at large angles to the jet axis (e.g. Barthel 1989).

To understand the accretion mechanism(s) we need to understand orientation effects, especially in X-ray selected samples. In the simple picture of an obscuring torus, quasar light heats the gas and dust of the torus and thermal radiation is re-emitted isotropically in the mid/far-infrared in order to maintain energy balance in the inner regions. Thus, in principle, far-infrared radiation should provide an orientation-independent measure of the emitted power from the central engine. The sensitivity in the mid/far-infrared of the *Spitzer* satellite provides for the first time the possibility to test this hypothesis for a large number of objects.

On larger spatial scales, extended X-ray emission is observed from spatial regions coincident with the radio lobes, and the combination of the X-ray and radio radiation can be used to measure the particle content and magnetic field in the radio lobes. In addition, the well collimated relativistic jets associated with these sources, require a medium in which to propagate. As a result powerful high redshift radio galaxies are potential tracers of the formation and evolution of the most massive galaxies and clusters (e.g., Crawford & Fabian 2003; Hardcastle & Worrall 1999; Worrall et al. 2001). Powerful radio sources are thus key objects to understand the cosmological evolution of accretion/radiation mechanisms, relativistic effects and plasma physics in the early Universe (e.g., Brunetti et al. 2001; Hardcastle, Birkinshaw & Worrall 2001; Marshall et al. 2005; Overzier et al. 2005).

In this paper we present high-quality X-ray observations obtained with *Chandra* and *XMM-Newton* of 19 sources in the redshift range $0.5 < z < 1.0$, which are mostly part of a larger sample of Faranoff-Riley type II (FRII) radio galaxies and quasars currently being observed with *Spitzer*. We discuss the properties of the core and particle content of the radio lobes and we present preliminary results on the cluster-like environment of these sources.

Throughout this paper we use the concordance cosmology with $h_0 = H_0/100 \text{ km s}^{-1} \text{ Mpc}^{-1} = 0.7$, $\Omega_{\rm M} = 0.3$, $\Omega_\Lambda = 0.7$. If not otherwise stated, quoted errors are 1σ for one interesting parameter.

2. THE SAMPLE

Low-radio-frequency optically-thin synchrotron radiation from the radio lobes of radio-loud sources should be isotropic. Thus, selection of objects via their low-frequency radio emission represents the most reliable method for selecting an orientation-unbiased sample. The sample discussed in this paper is composed of 19 sources at redshift $0.5 < z < 1.0$, selected from the 3CRR catalogue (Laing, Riley & Longair, 1983) at 178 MHz, and having *Chandra* or *XMM-Newton* observations. This work does not aim at statistically testing unification models, for which a random selection from the parent sample would be necessary. Instead we intend to look for differences in the X-ray emitting components between quasars and radio galaxies, as would be expected in unification schemes. The sources are also being observed with *Spitzer* and their selection as part of a larger sample was based on convenient scheduling of *Spitzer* observations.

Chandra or *XMM-Newton* observations of 9 sources (3C 184, 3C 200, 3C 220.1, 3C 228, 3C 263, 3C 275.1, 3C 292, 3C 330, 3C 334) were awarded to us in support of various projects, while data for the remaining sources were extracted from the *Chandra* archive. Table 1 lists the sources used in this work. Our analysis of the lobe emission was performed with a larger sample, including sources at lower and higher redshift to those detailed in Table 1. For a full list of these sources see Croston et al. (2005).

3. THE PROPERTIES OF THE CORES

High-frequency nuclear radio emission probes subarcsecond scales of radio-loud sources, and is explained as synchrotron radiation from the unresolved bases of relativistic jets, which is anisotropic due to relativistic beaming. The correlation found using *ROSAT* data between the nuclear, soft X-ray emission and the core radio emission of powerful radio-loud AGN (e.g. Hardcastle & Worrall 1999; Brinkmann, Yuan & Siebert 1997) suggests that at least part of the soft X-ray emission is also relativistically beamed and originates at the base of the jet. The correlation is very tight for core-dominated quasars (CDQs), i.e. those source having jets pointing to small angles to the line of sight. Another subclass of object, lobe-dominated quasars (LDQs), were found to lie above the flux-flux correlation valid for CDQs (Worrall et al., 1994), supporting the idea that lobe-dominated quasars are viewed at an angle to the line of sight such that the observer sees in X-ray both the jet-dominated component and a more isotropically emitted, probably nucleus-related component, with the two components being more similar in flux density than for the CDQs. For those sources viewed on the plane of the sky (thus strongly obscured by a torus) the picture is less clear. Worrall et al. (1994) found that the core soft X-ray emission of the galaxy 3C 280 lies on an extrapolation of the correlation obtained for CDQs, and interpreted the result as due to X-ray emission from a jet-related component, with the nucleus-related component being obscured by a torus. In this picture, nucleus-related X-ray emission in radio galaxies would be seen only at hard (> 2.5 keV) energies and its characteristics have been essentially unknown before *Chandra* and *XMM-Newton* observations.

3.1. Results

Chandra and *XMM-Newton* observations allow us to answer some of the still open questions about the nature of X-ray emission from the nuclear region of high-redshift radio sources:

1. **Do RGs have more absorbed cores than QSOs?** Spectral analysis of 10 radio galaxies in the sample show that 70% of them display an absorbed nuclear component with intrinsic absorption ranging from 0.2 to 50 $\times 10^{22}$ cm^{-2}. We do not find absorption above Galactic value for any of the quasars in the sample.

2. **If soft X-ray emission is jet-related, a correlation should exist between core radio emission and a soft X-ray unabsorbed component of RGs and CDQs.**

   We correlate core radio luminosity density at 5 GHz to soft, 1-keV X-ray luminosity density of an unabsorbed component in all the sources in our sample (Figure 1). We confirm previous results found with *ROSAT* about the tight correlation valid for CDQs, and the position above the correlation for LDQs. The 1-keV emission from the 10 RGs, which is interpreted as jet-related in CDQs, lies above the correlation valid for CDQs, suggesting that the mechanism responsible for the unabsorbed X-ray emission in the two subclasses of sources may be different.

3. **Are the two populations (RGs and QSOs) different in their X-ray spectral properties?**

   Radio-loud (core-dominated or blazar-type) quasars are found to have flatter spectral index , i.e. $\Gamma \sim 1.5$ (e.g., Worrall & Wilkes 1990, Brinkmann et al. 2000) in comparison to the values of $\Gamma \sim 2$ more commonly found in their radio-quiet counterparts

Table 1. The sample. Galactic column density is from Dickey & Lockman (1990); NRLG means Narrow Line Radio Galaxy; LERG means low-excitation radio galaxy. Redshifts and positions are taken from Laing et al. (1983)

Source	RA(J2000) h m s	Dec(J2000) ° ′ ″	redshift	scale arcsec/kpc	type	$N_{\rm H}$ 10^{20} cm $^{-2}$
3C 6.1	00 16 30.99	+79 16 50.88	0.840	7.63	NLRG	14.80
3C 184	07 39 24.31	+70 23 10.74	0.994	8.00	NLRG	3.45
3C 200	08 27 25.44	+29 18 46.51	0.458	5.82	NLRG	3.7
3C 207	08 40 47.58	+13 12 23.37	0.684	7.08	QSO	4.1
3C 220.1	09 32 39.65	+79 06 31.53	0.61	6.73	NLRG	1.8
3C 228	09 50 10.70	+14 20 00.07	0.552	6.42	NLRG	3.18
3C 254	11 14 38.71	+40 37 20.29	0.734	7.28	QSO	1.90
3C 263	11 39 57.03	+65 47 49.47	0.656	6.96	QSO	1.18
3C 265	11 45 28.99	+31 33 49.43	0.811	7.54	NLRG	1.90
3C 275.1	12 43 57.67	+16 22 53.22	0.557	6.40	QSO	1.99
3C 280	12 56 57.85	+47 20 20.30	0.996	8.00	NLRG	1.13
3C 292	13 50 41.95	+64 29 35.40	0.713	6.90	NLRG	2.17
3C 309.1	14 59 07.60	+71 40 19.89	0.904	7.80	GPS-QSO	2.30
3C 330	16 09 34.71	+65 56 37.40	0.549	6.41	NLRG	2.81
3C 334	16 20 21.85	+17 36 23.12	0.555	6.38	QSO	4.24
3C 345	16 42 58.80	+39 48 36.85	0.594	6.66	core-dom QSO	1.13
3C 380	18 29 31.78	+48 44 46.45	0.691	7.11	core-dom QSO	5.67
3C 427.1	21 04 06.38	+76 33 11.59	0.572	6.49	LERG	10.90
3C 454.3	22 53 57.76	+16 08 53.72	0.859	7.68	core-dom QSO	6.50

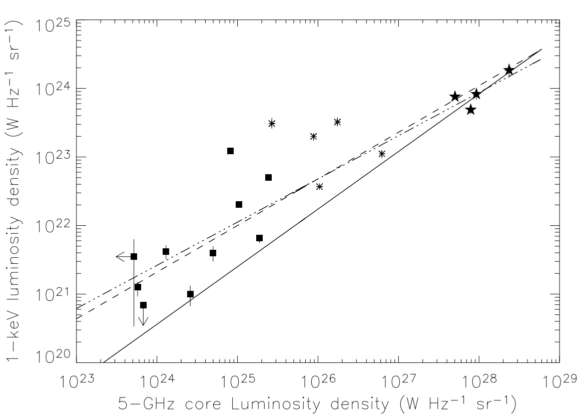

Figure 1. Luminosity-Luminosity relation. Filled boxes are RGs, asterisks are LDQs and star CDQs. Errors bars show 1σ uncertainties. When these are not visible it is because errors are smaller than symbols. Upper limits are at the 3σ level. The continuous line is the best-fit regression to the sample of CDQs only. The dot-dashed line is the regression to the whole sample, while the dashed line fits the sample composed of CDQs and RGs

(e.g. Brinkmann et al. 2000, Reeves & Turner 2000, Galbiati et al. 2005). The flat spectrum has been interpreted as the result of beamed emission from the jet. However, for RGs it is in principle possible to separate X-ray emission which is unobscured and jet-related from obscured (possibly) accretion-related emission. From our analysis we find that the average spectral index (Figure 2; the absorbed component is here considered for RGs) for all sources is $<\Gamma>$ = 1.55 ± 0.05, for RGs alone is $<\Gamma_{RG}>$ = 1.57 ± 0.03, for CDQs $<\Gamma_{CDQ}>$ = 1.45 ± 0.06, and for LDQs $<\Gamma_{LDQ}>$ = 1.59 ± 0.09. This shows that RGs absorbed emission behaves more similarly to the spectral behaviour of radio-loud quasars (RLQs) than radio-quiet quasars (RQQs).

Interestingly, the spectral index of the RG unabsorbed X-ray emission at low energy is rather steep, with a average of $<\Gamma>$ = 2.05 ± 0.25. This is indication that the emission mechanism responsible for the unabsorbed emission in RGs and QSOs may be different.

3.2. Conclusions

Several results support a simple unification model to explain the X-ray emission from high-redshift radio loud sources:

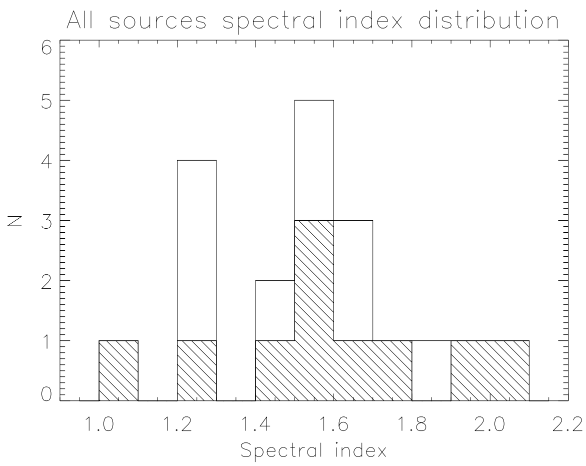

Figure 2. Spectral index distribution for the whole sample. The dashed histogram illustrates the distribution of the absorbed components of radio galaxies, and empty boxes represent quasars.

- RGs display higher intrinsic absorption than QSOs (as expected if a torus is present);
- the unabsorbed X-ray component observed in RGs (and QSOs) correlates with the radio core, implying that this emission is most likely jet related. However the steeper spectrum observed in RGs is consistent with synchrotron emission as the mechanism responsible for this emission in RGs. On the other hand,
- the flattening of the flux-flux relation (as well as the luminosity-luminosity relation) for CDQs, i.e. the source is under-luminous in X-ray for a given radio flux, is consistent with IC becoming dominant with decreasing angle to the line of sight;
- LDQs have more X-ray emission than would be expected from a jet component alone suggesting a possible contribution to the spectrum from both jet-related and accretion-related emission mechanisms.

The new and surprising result we find from our analysis is the flat slope describing the absorbed X-ray spectrum of RGs. In particular its value is flatter than that observed for RQQs. This seems to indicate that jet emission dominates over a possible more heavily absorbed core, as verified by simulations (Belsole, Worrall & Hardcastle, 2006). However, we cannot rule out that RLQs and RQQs engines are different.

4. EXTENDED EMISSION FROM THE RADIO LOBES

Radio synchrotron emission from radio lobes is a function of electron density and magnetic field strength. The combination of radio observations with resolved X-ray observations allows us to decouple these two quantities since electron density is directly measurable from the inverse Compton (IC) emission observed in the X-rays. This may help in solving the issue of particle content and magnetic field strength in radio lobes.

The particle content in radio galaxies and quasars is still under debate. Possible interpretations are electron-proton jets (e.g., Celotti & Fabian 1993) and electron-positron jets (e.g., Wardle et al. 1998; Kino & Takahara 2004). Although relativistic protons are not directly observable by IC emission, results consistent with equipartition between the magnetic field and electron energy densities represent an indirect means to disfavour models in which a substantial contribution to the energy density is provided by a population of protons (e.g., Hardcastle et al. 2004; Croston et al. 2004).

In this paper we summarise the results obtained from the analysis of *Chandra* and *XMM-Newton* observation of 33 classical double radio galaxies and their radio lobes. Detail of this work are described in Croston et al. (2005).

4.1. Results

The X-ray observations available allow us to resolve emission from 38 lobes and upper limits for another 16 lobes. Of the 38 lobes with detection, 8 have sufficient counts to perform spectral analysis.

The properties of the lobes in our sample were investigated by computing the ratio (R) of the observed to predicted X-ray flux at equipartition. The predicted flux was obtained by modelling of the IC and synchrotron emission using the radio flux densities at different frequencies to normalise the synchrotron spectrum. A broken power law electron distribution with initial electron energy index $\delta = 2$, $\gamma_{\rm min}$ =10 and $\gamma_{\rm max} = 10^5$, and a break energy in the range $\gamma_{\rm break} = 1200 - 10,000$ was used. The prediction for the CMB IC and SSC at 1 keV was determined on the basis of the modelled synchrotron spectrum for each source assuming equipartition between radiating particles and magnetic field. In this definition $R = 1$ means that the CMB and SSC model with an equipartition magnetic field and a filling factor of unity can explain the observed X-ray flux. $R > 1$ indicates that either the magnetic field is lower than the equipartition value, i. e., the lobes are electron dominated, or an additional photon field is present. $R < 1$ implies magnetic field domination.

Figure 3 shows the histogram of R for the detected lobes. The majority of sources have $R > 1$ and appear to be distributed around $R \sim 2$.

We also examined whether the observed R-value is related to the type of radio source by comparing the distribution of R for narrow-line and broad-line objects. We observe that broad-line quasars have a tendency to display higher value of R (Figure 3). We demonstrated (Croston et al., 2005) that projection effects are likely

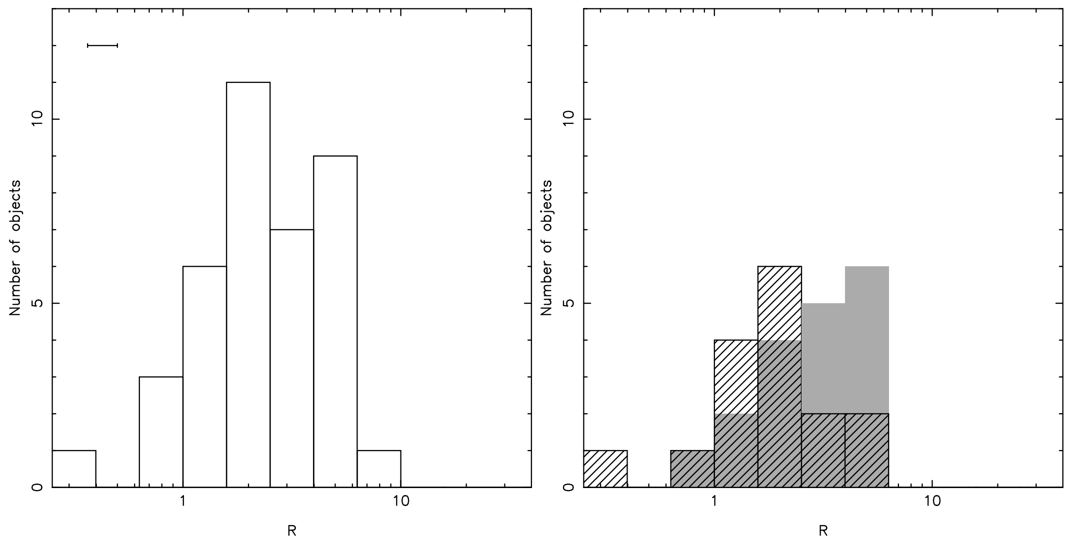

Figure 3. Distribution of R-parameter for the detected lobe sample (Left), and R distribution of the narrow-line (hatched rectangles) and broad line (filled rectangles) objects discussed in Croston et al. (2005) (Right).

to be important in explaining the distribution of the observed R-values, although other possibilities cannot be ruled out.

4.2. Conclusions

Our study shows that more than 70% of the sources in the sample are at equipartition or electron dominated. The distribution of the R-values, with a peak around $R \sim 2$ indicates that most of the source magnetic fields are within 35% of equipartition, or electron dominance (U_e/U_b) by a factor of ~ 5. Some sources can be magnetically dominated by at least a factor of 2. These results disfavour models in which FRII lobes have an energetically dominant population of relativistic protons which are also in equipartition with the magnetic field.

5. ENVIRONMENT OF RADIO SOURCES AND THE SEARCH OF HIGH-REDSHIFT CLUSTERS

Because of the propagation of radio jets, radio galaxies are expected to lie in an external medium dense enough to confine their relativistic jets. The combination of this hypothesis with the visibility of radio galaxies at high redshift suggested that these objects can be used as tracers of high-redshift galaxy clusters, by looking for hot intracluster medium around them in X-rays.

Observations with the *ROSAT* satellite were promising in this context (e.g., Crawford & Fabian 1993; Worrall et al. 1994; Crawford et al. 1999; Hardcastle & Worrall 1999), with detection of cluster-like emission around some of the $z > 0.5$ sources in the 3CRR catalogue.

Chandra and *XMM-Newton* make it now possible to detect and study the environment of high redshift radio galaxies in great detail, and to separate spatially and spectrally the different components (core, lobes, jets) responsible for the X-ray emission from these sources. The picture from *Chandra* and *XMM-Newton* is rather different from that of previous satellites.

5.1. The current picture: results from *Chandra* and *XMM-Newton*

Preliminary results for sources analysed so far are shown in Figure 4. Published work in the literature, and here assembled, shows that most of the radio galaxies and quasars in the redshift range $0.5 < z < 1.0$ show a tendency to lie in extended environments with luminosities of few $10^{43} h_{70}^{-2}$ erg s^{-1} (e.g. Hardcastle et al. 2002; Crawford & Fabian 2003; Donahue, Daly & Horner 2003; see Fig. 4). Only few objects have been confirmed spectroscopically (3C220.1 - Worrall et al. 2001, 3C184 and 3C292 - Belsole et al. 2004). Indeed most of the X-ray emission associated with these and other sources was found to be elongated in the direction of the radio lobes (Carilli et al., 2002; Hardcastle et al., 2002; Donahue, Daly & Horner, 2003; Croston et al., 2005)

Despite the low surface brightness emission from these objects, most of these environments are sufficient to confine the radio lobes (e.g. Hardcastle et al. 2002; Donahue, Daly & Horner 2003; Belsole et al. 2004).

The preliminary picture we observe from our study is suggesting that radio sources at high redshift trace a particular type of environment, i.e. they prefer poor environments at high redshift. This also supports that they may represent a means to built up a more unbiased sample for

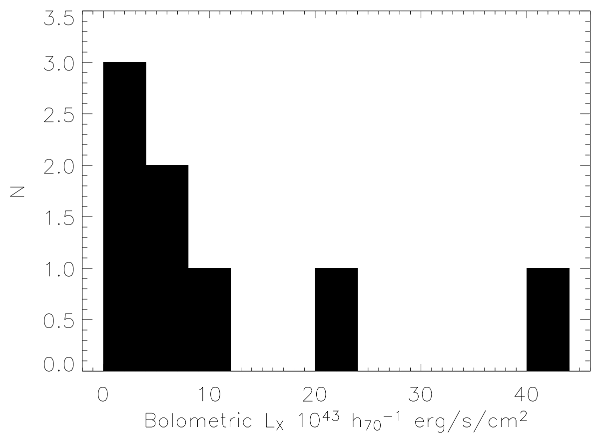

Figure 4. Distribution of the bolometric X-ray luminosity of 3CRR sources with detected extended, cluster-like emission.

structures in the high-redshift Universe, where massive clusters are expected to be fewer in the hierarchical formation paradigm.

This calls for a systematic study of a well selected sample of radio sources, and the 3CRR catalogue is a good starting point.

Work on the detection of extended emission from the sources in Table 1 is under way. Our full study will allow us not only to probe the characteristics of the extended emission, but also to constrain the physical state of the radio source itself by comparing the internal and external pressure of the radio lobes.

ACKNOWLEDGEMENTS

We are very grateful to the organisers of this conference for allowing us to present the work described in the paper. This well-organised meeting was enjoyable for the richness of results presented. This paper is based on observations obtained with *XMM-Newton*, an ESA science mission with instruments and contributions directly funded by ESA Member States and the USA (NASA). This research has made use of the NASA's Astrophysics Data System.

REFERENCES

Barthel P.D., 1989, ApJ, 336, 606

Belsole, E., Worrall, D.M., Hardcastle, M.J., Birkinshaw, M., Lawrence, C.R., 2004, MNRAS, 352,924

Belsole,E., Worrall, D.M., Hardcastle, M.J., 2006, MNRAS, submitted

Brinkmann W., Yuan W., Siebert J., 1997, A&A, 319, 413

Brinkmann W., Laurent-Muehleisen S. A., Voges W., Siebert J., Becker R. H., Brotherton M. S., White R. L., Gregg M. D., 2000, A&A, 356, 445

Brunetti, G., Cappi, M., Setti, G., Feretti, L., Harris, D. E., 2001, A&A, 372, 755

Carilli, C. L., Harris, D. E., Pentericci, L., Röttiger, H. J. A., Miley, G. K., Kurk, J. D., van Breugel, W., 2002, ApJ, 567, 781

Celotti, A. & Fabian, A.C, 1993 MNRAS, 264, 228

Crawford, C. S. & Fabian, A. C., 1993, MNRAS, 260, 15

Crawford, C. S., Lehmann, I., Fabian, A. C., Bremer, M. N., Hasinger, G.,1999, MNRAS, 308,1159

Crawford, C. S. & Fabian, A. C., 2003, MNRAS, 339, 1163

Croston J.H., Birkinshaw M., Hardcastle, Worrall D.M., 2004, MNRAS, 353, 879

Croston J.H., Hardcastle M. J., Harris D. E., Belsole E., Birkinshaw M., Worrall, D.M., 2005, ApJ, 626,733

Dickey J.M. & Lockman F.J., 1990, ARA&A, 28, 215

Donahue, M., Daly, R. A., Horner, D. J., 2003, ApJ, 584, 643

Galbiati E., et al., 2005, A&A, 430, 927

Hardcastle, M. J., Worrall, D. M., 1999, MNRAS, 309, 969

Hardcastle M. J., Birkinshaw M., Worrall D. M., 2001, MNRAS, 326, 1499

Hardcastle, M. J., Birkinshaw, M., Cameron, R. A., Harris, D. E., Looney, L. W., Worrall, D. M., 2002, ApJ, 581, 948

Hardcastle, M.J., Harris, D.E., Worrall, D.M., Birkinshaw, M., 2004, ApJ, 612, 729

Kino, M., & Takahara, F., 2004, MNRAS, 349, 336

Laing R. A., Riley J. M., Longair M. S., 1983, MNRAS, 204, 151

Marshall H. L., et al., 2005, ApJS, 156, 13

Overzier, R. A., Harris, D. E., Carilli, C. L., Pentericci, L., Röttgering, H. J. A., Miley, G. K., 2005, A&A, 433, 87

Reeves J.N. & Turner M.J.L., 2000, MNRAS, 316, 234

Urry C. M. & Padovani P., 1995, PASP, 107, 803

Wardle, J.F.C, Homan, D.C., Ojha, R., Roberts, D.H., 1998, Nature, 395, 457

Worrall D.M. & Wilkes B.J., 1990, ApJ, 360, 396

Worrall, D. M., Lawrence, C. R., Pearson, T. J., Readhead, A. C. S., 1994, ApJ, 420, L17

Worrall, D. M., Birkinshaw, M., Hardcastle, M. J., Lawrence, C. R., 2001, 326, 1127